

M. J. Burin · H. Ji · E. Schartman · R. Cutler  
P. Heitzenroeder · W. Liu · L. Morris  
S. Raftopolous

## Reduction of Ekman circulation within Taylor-Couette flow

Received: 28 July 2005 / Revised: 30 December 2005 / Accepted: 13 February 2006 / Published online: 24 March 2006  
© Springer-Verlag 2006

**Abstract** We demonstrate experimentally that independently rotating intermediary end-rings between the cylinders of a Taylor–Couette apparatus can be utilized to reduce friction-driven secondary flow, i.e. Ekman circulation. This allows for velocity profiles in a device of small aspect ratio to be less constrained by ‘end effects’, so that the resulting wide-gap flows can be made to have a radial distribution of circumferential velocity that resembles a narrow-gap Couette solution.

### List of symbols

$\Omega_{1(2)}$	rotation rate of the inner (outer) cylinder
$\eta$	radius ratio, $r_1/r_2$ , where $r_{1(2)}$ is the radius of the inner (outer) cylinder
$\Gamma$	aspect ratio, $H/(r_2 - r_1)$ , where $H$ is the height of the cylinders
$Re$	Reynolds number, $Re \equiv \frac{\Omega r (\Delta r)}{\nu}$ , where $\Omega$ is the rotation rate, and $\Delta r = r_2 - r_1$ .

### 1 Introduction

The Taylor–Couette system of fluid motion between two differentially rotating concentric cylinders enjoys a long and celebrated history (see e.g. Tagg 1994 and references therein). A majority of work done in this system is in the

narrow gap limit, i.e. with large aspect ratios. In this limit the vertical boundaries (or end-caps) between the cylinders do not have a dynamical role, even with finite viscosity. G.I. Taylor’s seminal work on viscous centrifugal instability (1923) utilized aspect ratios exceeding 100 for this reason. Experiments with smaller aspect ratios and relatively wide gaps (with  $\Gamma$  of order 10 and less) are somewhat less common, but apply to numerous engineering applications, such as computer hard-drives and other various turbomachinery (e.g. Schuler et al. 1990).

Secondary flows are important in small aspect ratio devices, and have their origin with the development of boundary layer inflow or outflow. The mechanism generating these boundary-driven flows is straightforward, as the no-slip condition at the end-cap surfaces (which are typically coupled to the outer cylinder) does not allow for pressure forces to be balanced centrifugally. Consequently, the resulting imbalanced pressure gradient near the boundaries drives a radial flow. Figure 1 gives a sketch of this phenomenon in the context of our experimental conditions. This secondary flow that develops within differentially rotating cylinders can be considered to be analogous to geophysical Ekman flow, and is part of the family of rotating boundary layer flows which includes Von Kármán and Bödewadt flows (White 1991). Ultimately, in an incompressible fluid, the boundary flow creates a meridional circulation in the  $r$ – $z$  plane, i.e. Ekman cells. At lower  $Re$  the cells are usually symmetric about the mid-plane, though asymmetry can develop at higher Reynolds numbers where the Taylor instability can play a role (e.g. Lücke 1984; Pfister et al. 1988). The work of Benjamin (1978) spurred appreciable interest, both theoretically and experimentally, on how end-cap boundaries in small  $\Gamma$  flows affect the various instability sequences and regimes that have been long recognized and investigated in narrow-gap flows. Some more recent work has investigated the dynamics of Ekman cells with regard to their interaction with the Taylor instability (Sobolik et al. 2000; Czarny et al. 2003).

M. J. Burin (✉) · H. Ji · E. Schartman · R. Cutler  
P. Heitzenroeder · W. Liu · L. Morris · S. Raftopolous  
Princeton Plasma Physics Laboratory, Princeton University,  
Princeton, NJ, USA  
E-mail: mburin@princeton.edu  
E-mail: hji@pppl.gov

M. J. Burin  
Department of Astrophysical Sciences, Princeton University,  
Princeton, NJ, USA

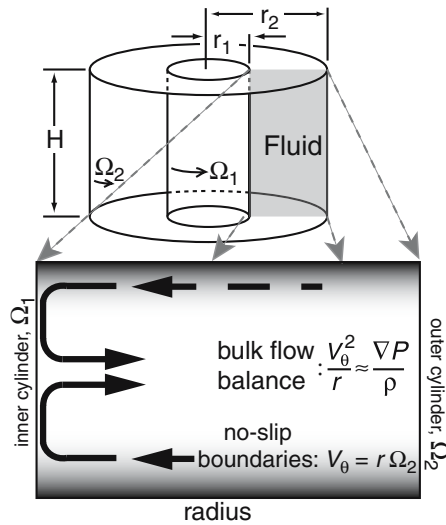


**Fig. 1** Schematic of the experimental geometry (not to scale) and cross-section illustrating heuristically the end-cap boundary inflow that induces Ekman circulation in a small aspect ratio Taylor–Couette apparatus

Ekman flows distort the simple analytic radial dependence for circumferential velocity found for the narrow-gap limit, i.e. the solution first derived by Couette (1890):  $V_\theta = Ar + B/r$ , where  $A$  and  $B$  are constants solely dependent on the rotation speeds and radii of the cylinders. That is, the Couette profile (which results from a purely viscous and constant radial flux of angular momentum) does not take into account boundary layer driven transport, e.g. Ekman circulation, which can significantly alter the primary flow via a redistribution of angular momentum (and vorticity). The distorting effects of Ekman circulation upon the ideal Couette velocity profile were examined by Coles and Van Atta (1966). These effects are understandably more severe for small aspect ratios, and recent numerical and experimental work by Kageyama et al. (2004) in a very short annulus ( $\Gamma \sim 1$ ,  $\eta \sim 0.25$ ) illustrate this fact. In their apparatus (with  $Re \sim 10^6$ ) the flow was observed to have a circumferential velocity profile that, due to the aforementioned redistributing effects of the Ekman circulation, is nearly flat over radius. The ultimate motivation in that study, and ultimately with ours, is to produce radial profiles that are practically free from end-effects, and so produce profiles near Couette’s narrow-gap solution, but in a wide-gap apparatus. This flow control is an essential step in a new experimental program studying high- $Re$  centrifugally-stable shear flows in an effort to model in the laboratory the inferred hydrodynamic and magnetohydrodynamic properties of astrophysical accretion disks. Such disks typically possess positive angular momentum gradients (i.e. increasing outwards) along with negative angular velocity gradients. For more information on this motivation, see e.g. Richard and Zahn (1999) and Ji et al. (2001).

As a way to practically reduce Ekman circulation, Kageyama et al. (2004) proposed multiple independent end-rings between inner and outer cylinders, to rotate at intermediary speeds. Their numerical results showed that just a couple rings would be adequate to prevent significant Ekman circulation from forming (or, to adequately shear it apart). This intermediary end-ring design is a novel approach to increase control over the velocity profile by an increased number of boundary conditions. It can be considered both a hybrid and a step beyond the split end-cap design (e.g. Wendt 1933), where the inner half of the end-caps rotates with the inner cylinder and the outer half rotates with the outer cylinder, and the independently rotating end-caps recently utilized by Abshagen et al. (2004). Guided by such innovations, and especially the work of Kageyama et al. (2004), we have constructed a modified Taylor–Couette device having the proposed intermediary end-rings. In Sect. 2, we discuss the design of this new apparatus, while in Sect. 3 we review some preliminary data which exemplify the effectiveness of the rings in controlling the velocity (and thereby momentum) distribution within the annulus, reducing Ekman circulation and thus achieving Couette-like flow profiles.

## 2 Apparatus and data acquisition

A schematic of the rotating components of our experimental apparatus may be seen in Fig. 2b, which is contrasted with a traditional Taylor–Couette arrangement in Fig. 2a. A more detailed drawing of the apparatus is provided in Fig. 2c. The apparatus is essentially a Taylor–Couette device where the annular area between the inner and outer cylinders has been modified to accommodate two intermediary end-rings at both vertical boundaries. Fluid is put into and withdrawn from the vessel with a simple pump and quick-connect<sup>®</sup> fitting. All rotating components of the primary vessel are composed of cast acrylic, with the exception of the inner cylinder, which is stainless steel. The outer radius of the inner cylinder and the inner radius outer cylinder are 7.06 and 20.30 cm, respectively, and the height of the annulus is 27.86 cm. These dimensions give  $\Gamma \sim 2$  and  $\eta \sim 0.3$ . The radial width of both rings is about 6.4 cm. Gaps between all rotating components within the vessel are about 0.15 cm. Though in principle the four rings can be driven independently, we have coupled the lower and upper rings together so that vertical boundary conditions are the same.

Each of the six rotating components is driven by a motor via a belt and pulley attached to a stainless steel shaft directly connected to the component. Between shafts are housings for PTFE (Teflon) seals, which prevent leaking of fluid from the relatively high-pressure environment within the rotating apparatus below, which can reach up to a few atmospheres with water as the working fluid. Seal and shaft diameter tolerances are

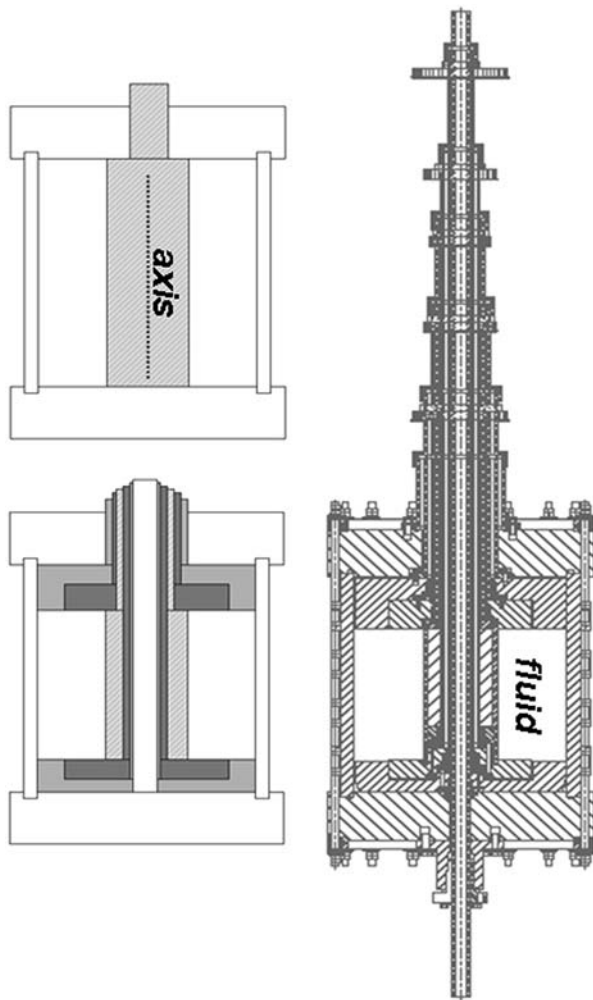


**Fig. 2** a Schematic of a typical Taylor–Couette device contrasted with b, a schematic of our modified design (to scale) featuring the addition of independently rotating intermediary end-rings between the inner and outer cylinders. In both schematics the level of shading corresponds to components which rotate at the same speed. c Drawing of the whole experimental apparatus, illustrating the six inter-nested drive shafts

0.005 cm. The seals are ‘energized’, that is having springs backing the sealing lip for additional pressure. Finding an appropriate spring strength, so that inter-shaft friction was minimized, while maintaining adequate sealing, was an iterative design process. Pressure differences between shafts due to different fluid levels are alleviated with small holes.

Radial alignment for each component is accomplished in two ways. Outside of the vessel, each shaft is clamped (via a split collar, which also provides axial support) to the inner diameter of a low profile 4-point angular contact ball bearing. Sleeve bearings machined from Techtron HPV<sup>®</sup> maintain radial alignment within the vessel. To remain within the wear rating of the bearing material, and to minimize vibrations, all rotating components were balanced to minimize radial loading. This entailed tight balancing tolerances (ISO

standard 1940-1 grade 2.5, typical of turbomachinery) for all rotating components, both individually and as an ensemble. Shaft radial alignment is accurate to 0.02 cm. Overall, the machining, sealing, and alignment of the inter-nested shafts proved to be mechanically nontrivial. The whole rotating apparatus is housed in a robust frame, which itself can be rotated to expedite maintenance. Temperature and vibration sensors can be monitored during experimental operations to ensure consistency of operating conditions.

Velocity data from within the fluid was obtained via dual-beam Laser Doppler Anemometry (LDA). Information on this technique can be found in the recent book by H.-E. Albrecht et al. (2003). For particles we utilized silvered glass beads approximately 14  $\mu\text{m}$  in diameter and with a density of 1.7 g/cc. To account for the optical effects introduced by the curved acrylic walls of the apparatus, data was calibrated empirically at known locations within the fluid under conditions of solid body rotation. LDA produces a series of velocity measurements from a small ellipsoidal measurement volume within the fluid. The major and minor axes of this measurement volume for this experiment were approximately 7 mm (radial) by less than 1 mm (azimuthal). Although the data series is unevenly sampled, estimates of the mean and r.m.s. obtained from the data are adequate for practical purposes.

To obtain data we utilized the following procedure. After starting rotation and allowing time for fluid spin-up (which is on the order of a minute), we scanned the fluid radially, obtaining velocity estimates at each radial position for approximately 30 s, which typically yielded  $10^3$  data points. The rotation of the apparatus was steady for the full scan (to within drive accuracy, about  $\pm 2$  r.p.m.). At a later time, the entire process was repeated at least once to ensure consistency of results.

### 3 Discussion of results

We have investigated the fitness of our design by assessing the effect of the intermediary end-rings. This was accomplished by first having both end-ring velocities set to the outer cylinder velocity, so that in effect the rings are not independent, but are coupled to and rotate with the outer cylinder, as in most Taylor–Couette devices. Data from this typical arrangement is compared with data obtained in a differential arrangement, i.e. with the inner and outer rings set at velocities independent of the inner and outer cylinder velocities. Velocity data from both types of rotation arrangement is presented in Fig. 3. It is clear that the end-rings have a significant effect on the flow. For the case with the rings coupled to the outer cylinder, the velocity profile is uniformly lower than the Couette solution, as can be expected considering Ekman circulation. By comparison, when the end-rings are activated, the velocity profile is much more Couette-like, suggesting that the Ekman circulation has been effectively reduced. We note that all

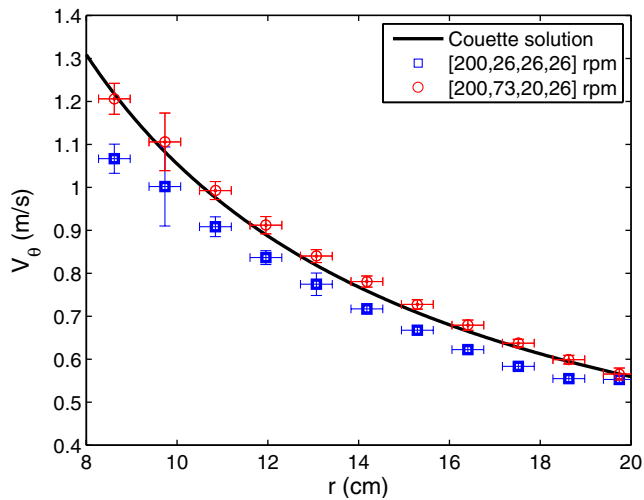


**Fig. 3** LDA results indicating the effectiveness of the independent end-rings in reducing Ekman circulation, as reflected in the radial distribution of circumferential velocity. Data from the fluid with the rings coupled to the outer cylinder (200, 26, 26, 26 r.p.m.) is contrasted with data with the rings rotating differentially (200, 73, 20, 26 r.p.m.). The analytic solution of Couette is given for comparison. *Vertical errors* are velocity r.m.s. while *horizontal errors* represent the positional uncertainty due to a finite measurement volume. Both data sets are from a height of 7.6 cm into the fluid from the bottom surface. The results are typical of all heights

data presented here is from a height of 7 cm ( $\pm 0.2$  cm) into the fluid from the bottom of the apparatus, a distance well outside of the estimated laminar boundary layer thickness of  $\delta \leq 1$  mm. Other heights within the fluid yield identical results.

The rotation rates for the two arrangements represented in Fig. 3 were chosen, from inner cylinder outwards, as [200, 26, 26, 26] r.p.m. and [200, 73, 20, 26] r.p.m. The first ('typical') regime was chosen to be at the border of centrifugal stability according to the (global) Rayleigh stability criterion. The latter ('differential') regime was arrived at empirically and iteratively. The starting point for the iteration was [200, 91, 33, 26] r.p.m., which was shown by numerical simulations (discussed below) to produce a near-Couette profile. Further study on the sensitivity of the flow to relatively small changes in the rotation rates of the boundaries is currently being pursued.

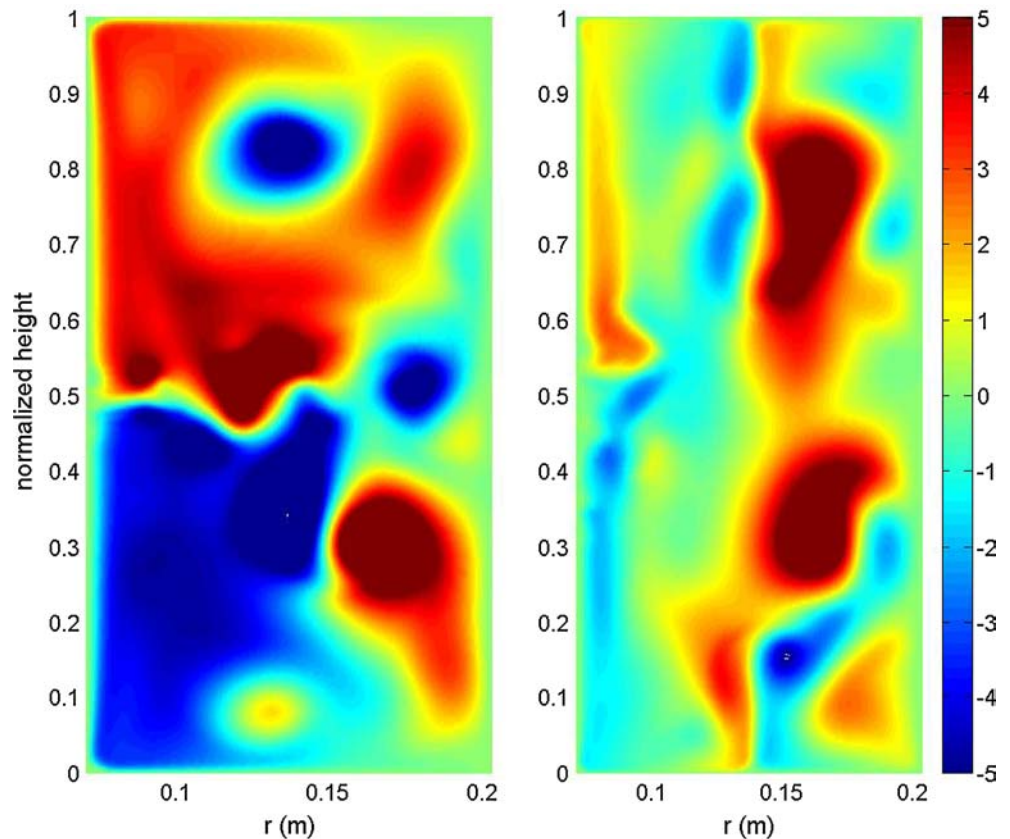
These experimental results are considered in light of numerical results from a 2D fluid simulation based on the Navier–Stokes equations with no-slip boundary conditions. In particular a grid ( $256^2$ ) representing the  $r$ – $z$  plane, having second-order spatial differences, is integrated temporally with a fourth-order Runge–Kutta method. Although rotation rates were accurately represented in this model, calculations necessarily included an artificially high viscosity, resulting in Reynolds numbers that are about a factor of 50 lower than experimental values. More detail on the model may be found in Kageyama et al. (2004).

Figure 4 gives representative streamfunctions from the 2D model for both rotation arrangements. This provides a good (though only qualitative) snapshot view of the difference caused by the independent end-rings. From the results described in Fig. 3 above, as well as numerous other studies, one would expect the typical rotation arrangement (with the end-rings coupled to the outer cylinder) to be significantly affected by Ekman circulation, and the left panel of Fig. 4 does indeed feature two large Ekman cells. Conversely, the differential case (as seen in the right panel) clearly shows a significant reduction of this circulation.

One may note the presence of two vortices over the outer ring ( $r > 0.14$  m) in the simulation of the differential conditions (Fig. 4, right panel). These areas of increased vorticity would likely be due in some part to centrifugal instability: though rotation conditions of the inner and outer cylinder satisfy the global centrifugal stability (Rayleigh) criterion  $[\Omega r^2]_1 < [\Omega r^2]_2$ , the *local* stability criterion  $\frac{d}{dr}[\Omega r^2] > 0$  is not met at the radii near the inter-ring boundary gap due to the abrupt change in speeds between the two closely-spaced rings. Thus even a small velocity decrease over the narrow ring gap should result in some centrifugal instability. However, despite this numerical prediction, we observe that the relative velocity r.m.s. levels in the fluid are both low (1–2%) and also homogenous throughout the fluid interior. Consequently we surmise that the predicted areas of increased vorticity are likely an artifact resulting from the relatively low Reynolds number of the simulation. The axisymmetry of the 2D simulations is also a possible cause for discrepancy. In any case, for now we shall defer further discussion of the fluctuation properties of these flows, as they will be discussed in future work.

In conclusion, we have shown that the presence of intermediary end-rings can significantly reduce Ekman circulation in a wide-gap Taylor–Couette device, allowing for velocity profiles like the (narrow-gap) Couette solution, for which end-effects are negligible. By increasing the number of boundary conditions, namely by splitting each end-cap into two independent rings, we have experimentally demonstrated an additional and effective control over the radial distribution of velocity, and hence momentum and vorticity, within the flow. The novel design we have implemented for this purpose also allows for a number of other studies, including possibly on the character of free-shear layers (i.e., Stewartson layers; Stewartson 1957) which should exist as circumferential sheets extending axially through the fluid from the inter-ring boundary. In a recent comment on our design (Hollerbach and Fournier 2004), it was pointed out that at the Reynolds numbers of our experiment ( $Re \sim 10^5$ ), these shear layers should penetrate into the fluid interior and create a small discontinuity in the velocity profile. The data near the ring-gap ( $r \sim 13.5$  cm), however, does not indicate any such discontinuity, though it may be that our resolution is inadequate for detecting it. If this is the case, higher

**Fig. 4** Qualitative view of the effect of end-rings as seen in typical instantaneous streamfunctions from a 2D numerical model. The *left panel* represents the case of the rings coupled to the outer cylinder, while in the *right panel* the rings rotate differentially, as in Fig. 3. The effective reduction of Ekman circulation is apparent



speed experiments (with  $Re > 10^6$ ) may yet reveal these layers. Alternately, one may suspect that mixing is occurring across the gap, allowing for a smooth radial profile across it. Interestingly, however, as mentioned above, the velocity across the gap in the fluid interior is accompanied by relatively low fluctuation levels, indicating that any mixing processes at work are nearly quiescent.

**Acknowledgments** This research was largely funded by the U.S. Department of Energy, grant DE-AC02-76-CH03073. MJB was supported from the NSF under grant AST-0205903. W. L. was supported under NASA grant ATP03-0084-0106 as well as NSF grant PHY-0215581, and he thanks A. Kageyama for providing the basis of a 2D fluid code whose results are featured in Fig. 4. The authors also thank C. Jun for additional engineering advice concerning the apparatus, as well as Dantec Dynamics for the contracted use of a LDA measurement system. Most of the manufacturing for the apparatus was provided by General Tool, of Cincinnati, OH, USA.

## References

- Abshagen J et al (2004) Taylor–Couette flow with independently rotating end plates. *Theor Comput Fluid Dyn* 18:129–136
- Albrecht H-E et al (2003) *Laser Doppler and Phase Doppler measurement techniques*. Springer, Berlin Heidelberg New York
- Benjamin TB (1978) Bifurcation phenomena in steady flows of a viscous fluid. *Proc R Soc Lond (I) Theory* 359:1–26, (II) *Experiments* 359:27–43
- Coles D, Van Atta C (1966) Measured distortion of a laminar circular Couette flow by end effects. *J Fluid Mech* 25:513–521
- Couette MM (1890) Etudes sur le frottement des liquides. *Ann Chim Phys* 21:433–510
- Czarny O et al (2003) Interaction between Ekman pumping and the centrifugal instability in Taylor–Couette flow. *Phys Fluids* 15:467–477
- Hollerbach R, Fournier A (2004) End-effects in rapidly rotating cylindrical Taylor–Couette flow. In: Rosner R et al (ed) *MHD Couette flows, experiments and models: AIP conference proceedings* 733, AIP press, Acitrezza, Catania, Italy, New York, pp 114–121
- Ji H et al (2001) Magnetorotational instability in a rotating liquid metal annulus. *Mon Not R Astron Soc* 325:L1–L5
- Kageyama A et al (2004) Numerical and experimental investigation of circulation in short cylinders. *J Phys Soc Japan* 73:2424–2437
- Lücke M et al (1984) Flow in a small annulus between concentric cylinders. *J Fluid Mech* 140:343–353
- Pfister G et al (1988) Bifurcation phenomena in Taylor–Couette flow in a very short annulus. *J Fluid Mech* 191:1–18
- Richard D, Zahn J-P (1999) Turbulence in differentially rotating flows: What can be learned from the Couette–Taylor experiment. *Astron Astrophys* 347:734–738
- Schuler CA et al (1990) On the flow in the unobstructed space between shrouded co-rotating disks. *Phys Fluids A* 2:1760–1770
- Sobolik et al (2000) Interaction between the Ekman layer and the Couette–Taylor instability. *Int J Heat Mass Transfer* 43:4381–4393
- Stewartson K (1957) On almost rigid rotations. *J Fluid Mech* 3:17–26
- Tagg R (1994) The Couette–Taylor problem. *Nonlinear Sci Today* 4:1–25
- Taylor GI (1923) Stability of a viscous liquid contained between two rotating cylinders. *Phil Trans R Soc Lond* 223:289–343
- Wendt F (1933) Turbulente strömungen zwischen zwei rotierenden konaxialen zylindren. *Ing Arch* 4:577–595
- White FM (1991) *Viscous fluid flow*. McGraw Hill, New York